

**CHEMISTRY 361**  
**QUANTUM CHEMISTRY**  
**AND**  
**CHEMICAL KINETICS**

**Enrique Peacock-López<sup>1,\*</sup>**

*<sup>1</sup>Department of Chemistry*

*Williams College*

*Williamstown, MA 01267*

(Dated: June 17, 2006)

**Abstract**

The early XX century saw the birth of the theory of relativity. This theory was developed after the 1887 Michelson and Morley's experiment which was designed to reveal the earth's motion relative to the ether. In an effort to explain the experimental facts, Poincare and Einstein altered the ideas and concept of space, time and astronomical distances. Most of the development of the theory of relativity was carried out by the latter scientists. In contrast Quantum chemistry took several decades and many contributors to be developed. This theory can be seen as an extension of classical mechanics to the subatomic, atomic and molecular sizes and distances.

In this course we will study the fundamental theory of electrons, atoms and molecules known as Quantum Chemistry. In our approach we will follow the historical development of Quantum Chemistry. In this approach we will see how Quantum Chemistry gradually evolves from confusion and dilemma into a formal theory.

---

\*Author to whom correspondence should be addressed. Electronic address: [epeacock@williams.edu](mailto:epeacock@williams.edu)

## Lecture 1

As we have seen in previous chapters, the world we experience with our senses is a world described by Thermodynamics, Classical Mechanics and Classical Electromagnetism. It is a macroscopic world based in macroscopic laws. But scientist have long recognized experimentally the existence of small particles which are the components of matter. Therefore it is natural to look first for microscopic laws that explain the particle's behavior, and second we have to look for a theoretical approach that will link the microscopic laws with the macroscopic laws.

Towards the end of the XIX century, many physicist felt that all the principles of physics had been discovered and little remained to be understood except for few minor problems. At that time our world was understood using Classical Mechanics, Thermodynamics and Classical Electromagnetism. For example in Classical Mechanics or Newtonian Mechanics we needed to find the dynamical variables of the system under study. Once done this, we needed to construct the equation of motion which predicted the system's evolution in time. The predicted behavior was finally compared with the experimental observations.

At the time the Universe was divided into matter and radiation. Matter was ruled by Newtonian mechanics and thermodynamics, and radiation obeyed Maxwell's laws of Electromagnetism. A controversy whether light was wave-like or corpuscular-like existed since Newton's days, who proposed the corpuscular theory of light. The wave-like theory was developed by Huggens based in the constructive and destructive interference of light; a property which is characteristic of waves.

The interaction between matter and radiation was not well understood. For example, Earnshaw's theorem states that a system of charged particles can not remain at rest in stable equilibrium under the influence of purely electrostatic forces. Moreover, according to Electromagnetism an accelerated charged particles radiate energy in the form. of electromagnetic waves. Thus how is that molecules are stable? From this minor problems the theory of Quantum chemistry was developed.

## Lecture 2

During the 17<sup>th</sup> century Galileo Galilei and Issac Newton postulated a corpuscular theory of light. After 200 years of work, in the 19<sup>th</sup> century we have a logical theory with deterministic equation that explain planetary motion as well as classical mechanics, thermodynamics, optics, electricity and magnetism.

In the mid 1800s, Thomas Young reported a pattern consisting of dark and bright fringes, which were produces after passing light through two narrow closely spaced holes or slits. This interference pattern is a natural wave behavior. By 1860, James Clark Maxwell developed a classical electromagnetic theory, which combines electricity and magnetism in a single theory. Also, Maxwell's theory predicts that the properties of light can be explained if we consider light as electromagnetic radiation. The experimental confirmation of maxwell equation was reported by Michael Faraday, and 1886, although assuming a luminiferous (ether) medium, Hertz confirmed experimentally that light is electromagnetic radiation giving the wave theory of light a solid foundation.

In 1887, Albert Michelson and edward Morley'1860, confirmed experimentally the electromagnetic waves traveled in vacuum by finding no difference in the speed of light relative to the motion of Earth. In other word, there is no need of the luminiferous or any other medium. Without a medium, light is subject to a relativistic description that was developed by Poincarè and Einstein.

From the classical Maxwell equations, we can prove Earnshaw's Theorem, which states that a system of charged particles can not remain at rest in stable equilibrium under the influence of purely electrostatic forces. In other words, accelerated charged particles radiate energy in the form of electromagnetic waves. So how atoms and molecules are stable? or how atoms and molecules absorb and emit radiation **only** at certain frequencies?

### Electromagnetic waves

Electromagnetic waves are made up of an oscillating electric (**E**), and a perpendicular magnetic (**B**) and are produced by accelerated charges, where the electric field **E** displaces charged particles along the direction of the field, and the magnetic field **B** rotates charged particles around the direction of the field.

The electric field in units of volt  $m^{-1}$  and pointing in the Z-direction is described

$$E_z(y,t) = E_o \text{Sin}(k y - w t) \quad (1)$$

where the angular frequency is defined as

$$w = 2\pi\nu', \quad (2)$$

the wave vector as

$$k = \frac{2 \pi}{\lambda}, \quad (3)$$

and  $E_o$  is the amplitude of the electric field. The magnetic field pointing in the X-direction is described

$$B_x(y,t) = \frac{E_o}{c} \text{Sin}(k y - w t)', \quad (4)$$

where

$$\lambda \nu' = c = \frac{w}{k} \quad (5)$$

A single wavelength,  $\lambda$ , implies monochromatic light, where the range of wave lengths varies from:

$$\begin{array}{ccc} & \textit{Cosmic Rays} & \\ \lambda = 3 \cdot 10^{-24} \text{ m} & \nu = 10^{32} \text{ s}^{-1} & 4 \cdot 10^{17} \text{ eV} \\ & \updownarrow & \\ & \textit{Long radio waves} & \\ \lambda = 3 \cdot 10^6 \text{ m} & \nu = 10^2 \text{ s}^{-1} & 4 \cdot 10^{-13} \text{ eV} \end{array}$$

When Electro Magnetic radiations (light) interacts with matter, it gets scattered. In the case of scattering from many centers, we say that light gets diffracted. In contrast, when light gets scattered by few centers, we say that light shows interference.

## Lecture 3

### Blackbody radiation

Experimentally we observe that when a metallic object is heated it would change its color. As the temperature is increased, first the object changes its color into a dull red and, progressively, becomes more and more red. Eventually it changes from red to blue. As it is well established experimentally, the radiated energy is associated with a color which is associated to a frequency or wavelength. To understand this phenomenon, we will consider a so-called black-body

An ideal object that absorbs and emits all frequencies is defined as a black-body. It is a theoretical model invented by theorist to study the emission and absorption of radiation. Its experimental counterparts consist of an insulated box which can be heated. On one of its faces a small pinhole allows radiation to enter or leave. This radiation is equivalent to that of a perfect black-body.

One of the “minor” problems mentioned earlier relates to the density of radiated energy per unit volume per unit frequency interval  $d\nu$  at temperature  $T$ ,  $\rho(\nu, T)$ . The search for an expression for  $\rho(\nu, T)$  backs to 1860 when Gustav Kirchhoff recognized the need of a theoretical approach to blackbody radiation. Also the relation between  $\rho(\nu, T)$  with certain empirical equations was not well understood. In 1899 Wien noticed that the product of temperature,  $T$ , and maximum wavelength,  $\lambda_{max}$  was always a constant,

$$T \lambda_{max} = \text{constant}. \quad (6)$$

Equation 6 is called the displacement law. Also the total energy radiated per unit area per unit time,  $R$ , from a blackbody followed Stefan-Boltzmann law,

$$R = \sigma T^4, \quad (7)$$

where  $\sigma$  is a constant. These two empirical laws needed to be explained from first principles.

In 1896 Wilhelm Wien derived the following expression for  $\rho$ :

$$\rho(\nu, T) = C \nu^3 \exp\left\{-a \frac{\nu}{T}\right\}, \quad (8)$$

where  $C$  and  $a$  are constants. Wien's result was experimentally confirmed for high frequencies by Frederick Paschen in 1897. But in 1900, Otto Lummer and Ernest Pringsheim found

that Wien’s expression failed in the low frequency regime. The first attempts to explain

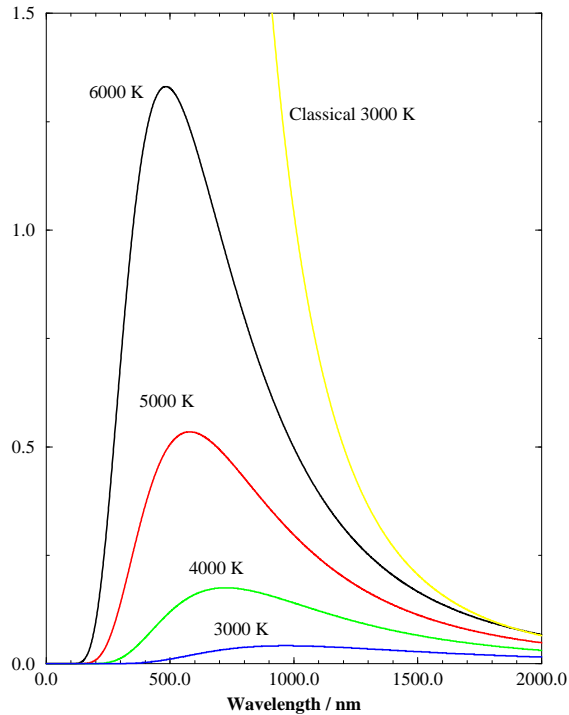


FIG. 1: Planck’s radiation density for a blackbody.

the previous empirical laws from first principles used the classical knowledge at the time. For example in 1900 Rayleigh assumed that the radiation trapped in the box interacted with the walls. On the walls small oscillators which in turn vibrate emitting radiation. Finally the equilibrium between the “oscillators” and the radiation trapped in the box is responsible of the properties of black-body radiation. Under these assumptions, the density of radiated energy per unit volume per unit frequency at temperature T is given by the following equation:

$$\rho(\nu, T) d\nu = N_\nu d\nu \bar{\epsilon}(\nu, T) , \quad (9)$$

where  $N_\nu d\nu$  represents the number of oscillators between  $\nu$  and  $\nu + d\nu$ , and  $\bar{\epsilon}(\nu, T)$  is the average energy radiated by the “electronic oscillator” at frequency  $\nu$  and temperature T. The number density was widely accepted to be

$$N_\nu = \frac{8\pi \nu^2}{c^3} \quad (10)$$

where  $c$  is the speed of light.

In the calculation of  $\bar{\epsilon}(\nu, T)$  Reyleigh assumed that the “oscillators” could achieve any possible energy and the equipartition theorem. In other words Rayleigh assumed a continuous energy spectrum for the oscillators and

$$\bar{\epsilon}(\nu, T) = k_B T , \quad (11)$$

where  $k_B$  is Boltzman constant. With these assumptions, Rayleigh obtained the following expression for the amount of radiative energy between  $\nu$  and  $\nu + d\nu$ :

$$\rho(\nu, T) d\nu = \frac{8\pi \nu^2}{c^3} k_B T d\nu . \quad (12)$$

If we express Eq. 12 as radiated energy per unit volume per unit wavelength we get

$$\rho'(\lambda, T) d\lambda = \frac{8\pi}{\lambda^4} k_B T d\lambda , \quad (13)$$

where we have used the relation  $c = \lambda\nu$ . This latter result agreed with the low frequency observation but did not fit the experimental observationsm at high frequencies.

From the low and high frequency expressions,

$$\bar{\epsilon}(\nu, T) \approx \begin{cases} k_B T & \text{for low } \nu \\ \nu \exp \left\{ - a \frac{\nu}{T} \right\} & \text{for high } \nu \end{cases} , \quad (14)$$

Planck derived an expression consistent with both limiting behaviors,

$$\bar{\epsilon}(\nu, T) = \frac{h \nu}{\exp \left\{ \frac{h\nu}{k_B T} \right\} - 1} . \quad (15)$$

This expression required only one constant,  $h$ , which Plank determined by fitting the expression to the experiemntal data. Equation 15 is called the Plank distribution law. Plank obtained an excellent agreement with experiments using

$$h = 6.626 \times 10^{-34} J s . \quad (16)$$

Although Eq. 15 fitted the experiemntal data extraordinary well, Plank wanted to understand why Eq. 15 worked so well. First Plank calculated the entropy of the system from 15. Second, he calculated the entropy using Boltzman mechanistic approach. When these two independent expression for the entropy were compared, Plank concluded the the oscillators

spectrum had to be discrete. In other words the “oscillators” could only achieve the following energy values:

$$\epsilon_n = n h \nu , \quad (17)$$

where  $n$  is a positive integer and  $h$  is Plank’s constant. Thus both of Plank’s entropy expression were consistent if energy was quantized.

From Max Planck’s underlying assumption that the energies of the “electronic oscillators” could have only a discrete set of values we can derive the semiempirical Plank’s distribution using statistical methods. In this approach we assumed that only jumps of  $\Delta n = \pm 1$  can occur, so the change of energy is given by:

$$\Delta\epsilon = h \nu . \quad (18)$$

This means that energy is absorbed or emitted only in packets.

In order to obtain an expression for the density of radiative energy between  $\nu$  and  $\nu + d\nu$  we have to calculate the average energy,  $\bar{\epsilon}(\nu)$ , at frequency  $\nu$ . First we consider the Boltzmann probability for the energy level of each oscillator at frequency  $\nu$ , i.e.,

$$P_n(\nu) \approx \exp \left\{ \frac{n h \nu}{k_B T} \right\} . \quad (19)$$

Using Eq. 19 we get for the average oscillator’s energy

$$\begin{aligned} \bar{\epsilon}(\nu) &= \frac{\sum_{n=1}^{\infty} n h \nu \exp \left\{ \frac{n h \nu}{k_B T} \right\}}{\sum_{n=1}^{\infty} \exp \left\{ \frac{n h \nu}{k_B T} \right\}} \\ &= \frac{\sum_{n=1}^{\infty} n h \nu X^n}{\sum_{n=1}^{\infty} X^n} \\ &= \frac{h \nu \frac{X}{(1-X)^2}}{\frac{1}{1-X}} \\ &= \frac{h \nu X}{1-X} \\ &= \frac{h \nu}{\exp \left\{ \frac{h \nu}{k_B T} \right\} - 1} . \end{aligned} \quad (20)$$

Finally using Eqs. 9 and 10 the Plank’s expression for the radiative energy density is equal to

$$\rho(\nu, T) d\nu = \frac{8\pi \nu^2}{c^3} \frac{h \nu}{\exp \left\{ \frac{h \nu}{k_B T} \right\} - 1} d\nu . \quad (21)$$

Also as a function of wavelength we get

$$\rho'(\lambda, T) d\lambda = \frac{8\pi hc}{\lambda^5} \frac{1}{\exp\left\{\frac{hc}{k_B T \lambda}\right\} - 1} d\lambda . \quad (22)$$

From Eq. 22 we can obtain the Wien displacement law and the Stefan-Boltzman law.

## Lecture 4

### Photoelectric effect

Late in the 19<sup>th</sup> century a series of experiments revealed that electrons are emitted from a metal surface when light of sufficient high frequency falls upon it. This is known as the photoelectric effect. Classical theory predicted that the energy of the ejected electron is proportional to the intensity of the light; electrons are ejected for any frequency radiated. Both prediction are not support by the experients.

The experiemnts show the existance of a threshold frequency,  $\nu_0$ . Einstein in 1905 assumed that radiation consists of little packets of energy  $\epsilon = h\nu$ . If this is true the kinetic energy of the ejected electron is given by the following equation:

$$KE = \frac{1}{2} mv^2 = h\nu - \phi \quad (23)$$

where  $\phi$  is the work function which is usually expressed in electron volts, eV. Note that the threshold frequency,  $\nu_0$ , implies no kinetic energy. Thus

$$h\nu_0 = \phi, \quad (24)$$

and the photoelectric effect is observed only if  $h\nu \geq \phi$ . Equation 23 represents a straight line with slope h. Actually in an experiment one measures the stopping potential,  $V_S$ , such that

$$KE = - e V_S = \frac{1}{2}mv^2 . \quad (25)$$

## Lecture 5

### Wave equation

In this section we discuss the wave equation for a string attached at both ends. In this case we consider a string along the x-axis with displacement in the y-direction. The string's displacement will be denoted as  $u(x,t)$ . Finally if we consider a string of length  $\ell$  the displacement satisfies the following equation:

$$\frac{\partial^2 u}{\partial x^2} = \frac{1}{v^2} \frac{\partial^2 u}{\partial t^2} , \quad (26)$$

where  $v$  is the magnitude of the velocity of the wave along the string. Next we consider the boundary conditions (BC). These are the values of  $u$  at the ends of the string. Since the ends are attached to say a wall, these points do not displace from its position,

$$u(0,t) = 0 = u(\ell,t) . \quad (27)$$

Notice that these values are valid for any time  $t$ . Thus we have a partial differential equation and its boundary conditions for a string. This equation is commonly referred as a 1-dimensional wave equation.

Of the different methods of solution of partial differential equations, we will consider the method of separation of variables. In this method we consider the the solution to Eq. 26 can be written as a product of a function of time and function of space, i.e.,

$$u(x,t) = X(x) T(t) . \quad (28)$$

If we substitute Eq. 28 in Eq. 26 we get

$$T(t) \frac{d^2 X(x)}{d x^2} = \frac{1}{v^2} X(x) \frac{d^2 T(t)}{d t^2} . \quad (29)$$

Notice that the partial derivatives have transformed to regular derivatives since they are applied to single variable function. Now if we divide both sides of Eq. 29 by Eq. 28 we get

$$\frac{1}{X(x)} \frac{d^2 X(x)}{d x^2} = \frac{1}{v^2 T(t)} \frac{d^2 T(t)}{d t^2} . \quad (30)$$

In Eq. 30 the left hand side is a function only of position  $x$ ; the right hand side is a function only of time. Since position and time are independent variables the only possibility that satisfies Eq. 30 is

$$\frac{1}{X(x)} \frac{d^2 X(x)}{d x^2} = \alpha , \quad (31)$$

$$\frac{1}{T(t)} \frac{d^2 T(t)}{d t^2} = \alpha , \quad (32)$$

where  $\alpha$  is a constant.

For the spatial function  $X(x)$  we have now the following equation:

$$\frac{d^2 X(x)}{d x^2} = \alpha X(x) \quad (33)$$

From Eq. 27 the boundary conditions for  $X(x)$  are

$$X(0) = X(\ell) = 0 . \quad (34)$$

Thus we are looking for a function that satisfies Eq. 33 and vanishes at  $x = 0$  and  $x = \ell$ . After some thinking we find that the function  $\sin(x)$  and  $\cos(x)$  satisfy the differential equation but only  $\sin(x)$  satisfies the boundary condition at  $x = 0$ . In other words, if

$$X(x) = A \sin(\kappa x) , \quad (35)$$

Eq. 33 reduces to

$$\begin{aligned} \frac{d^2 A \sin(\kappa x)}{d x^2} &= - A \kappa^2 \sin(\kappa x) \\ &= - \kappa^2 X(x) \\ &= \alpha X(x) . \end{aligned} \quad (36)$$

Therefore

$$\alpha = - \kappa^2 . \quad (37)$$

Next we consider the boundary condition

$$\sin(\kappa \ell) = 0 . \quad (38)$$

Equation 38 is satisfied if the argument of the sine function is an integer multiple of  $\pi$ ,

$$\kappa \ell = n \pi . \quad (39)$$

Solving for  $\kappa$  we find that the spatial solution of Eq. 26 to be

$$X(x) = A_n \sin\left(\frac{\pi}{\ell} n x\right) . \quad (40)$$

And the displacement  $u(x, t)$  can be written as

$$u_n(x, t) = T(t) A_n \sin\left(\frac{\pi}{\ell} n x\right) . \quad (41)$$

Equation 40 represents standing waves, and the wavelength of these standing waves,  $\lambda_n$  satisfy the following relation:

$$\frac{\pi}{\ell} n \lambda_n = 2\pi . \quad (42)$$

Thus  $\lambda_n$  is equal to

$$\lambda_n = \frac{2 \ell}{n} , \quad (43)$$

where  $n$  is an integer greater than one. Using this result we can express  $\kappa$  in terms of  $\lambda_n$ ,

$$\kappa = \frac{2 \pi}{\lambda} , \quad (44)$$

and plugg it in Eq. 31 to get the following equation:

$$\frac{d^2 X(x)}{d x^2} = - \left( \frac{2\pi}{\lambda_n} \right)^2 X(x) . \quad (45)$$

Equation 45 represents the wave equation satisfied by the spatial part of the amplitud,  $u(x, t)$ .

### Particle's wave equation

Since particles behave as waves we need a wave equation for a particle. A simple approach is to use de Broglie's assumption in Eq. 45. Namely we substitute the value of the wavelength associated to a particle with momentum  $p$ ,

$$\lambda = \frac{h}{p} , \quad (46)$$

in the right hand side of Eq. 45. This substitution yields the following equation:

$$\frac{d^2 \psi(x)}{d x^2} = - \left( \frac{p}{\hbar} \right)^2 \psi(x) , \quad (47)$$

where  $\psi$  is the wave associated to a particle with momentum  $p$  and  $\hbar \equiv h/2\pi$ . Now if we recall the expression for the mechanical energy of a particle with momentum  $p$  in a potential  $V(x)$ ,

$$E = \frac{p^2}{2 m} + V(x) , \quad (48)$$

and solve for  $p^2$  we get

$$p^2 = 2 m [E - V(x)] . \quad (49)$$

Equation 49 can be used in Eq. 47 and get

$$\frac{d^2 \psi(x)}{d x^2} = - \frac{2m}{\hbar^2} [E - V(x)] \psi(x) . \quad (50)$$

Finally we can rewrite Eq. 50 as

$$-\frac{\hbar^2}{2m} \frac{d^2 \psi(x)}{dx^2} + V(x) \psi(x) = E \psi(x) . \quad (51)$$

Equation 51 is the time-independent Schrödinger equation. Although this derivation is not formal, nor Schrödinger “official” derivation, it obtains the quantization of the energy, in the case of the hydrogen atom, as a consequence of the properties of the wave function  $\psi(x)$ . Schrödinger success attracted the attention of scientist and change the world.

### Schrödinger equation

$$-\frac{\hbar^2}{2m} \frac{\partial^2}{\partial x^2} \Phi(x, t) + V(x) \Phi(x, t) = i \hbar \frac{\partial}{\partial t} \Phi(x, t) . \quad (52)$$

Separation of variables

$$\Phi(x, t) = \phi(t) \psi(x) \quad (53)$$

$$-\frac{1}{\psi(x)} \frac{\hbar^2}{2m} \frac{d^2}{dx^2} \psi(x) + V(x) = \frac{i \hbar}{\phi} \frac{d}{dt} \phi(t) = \text{constant} = E \quad (54)$$

$$\frac{d \phi(t)}{dt} = -\frac{i E}{\hbar} \phi(t) \quad (55)$$

$$\phi(t) = \exp \left\{ -\frac{i E}{\hbar} t \right\} \quad (56)$$

$$-\frac{\hbar^2}{2m} \frac{d^2}{dx^2} \psi(x) + V(x) \psi(x) = E \psi(x) \quad (57)$$

## Lecture 6

### Axiomatic quantum mechanics

Classical mechanics deals with position ( $\vec{r}$ ), momentum ( $\vec{p}$ ), angular momentum ( $L \equiv mvr$ ) and energy. These quantities are called dynamical variables. A measurable dynamical variable is called an observable.

Time evolution of the system's observables is governed by Newton's equations, which yield the system's trajectory. In Quantum mechanics the Uncertainty Principle forbids the concept of trajectory. Thus we need another approach to study the microscopic world of the atom. In this section we consider an axiomatic approach. Namely we will state a number of axioms or postulates which define the foundation of quantum mechanics. The postulates are justified only by their ability to predict and correlate experimental facts and their general applicability.

#### 1. Postulate 1

The state of a quantum-mechanical system is completely specified by a function  $\Psi(\vec{r}, t)$ . This function is called the wave function or the state function.

The probability of finding the particle in a volume element  $dV$  around  $\vec{r}$  at time  $t$  is given by:

$$P(\vec{r}, t) = |\Psi(\vec{r}, t)|^2 dV = \Psi^*(\vec{r}, t) \Psi(\vec{r}, t) dV , \quad (58)$$

where the star,  $\Psi^*$  represents the complex conjugate of the wave function  $\Psi$ . As a consequence of the probabilistic interpretation, the probability of finding the particle some place in the space is equal to unity or

$$\int_{Space} |\Psi(\vec{r}, t)|^2 dV = 1 . \quad (59)$$

This condition puts some requirements on the kind of state function that we can consider. For example  $\Psi$  and  $d\Psi/d\vec{r}$  have to be continuous, finite and single-valued (for each position  $\vec{r}$  only one value of  $\Psi(\vec{r}, t)$ ).

## 2. Postulate 2

For any observable in classical mechanics, we can find a corresponding quantum mechanical operator. For example momentum in the x direction:

$$p_x = m v_x \longleftrightarrow \hat{p} = -i \hbar \frac{d}{dx}, \quad (60)$$

angular momentum in the x direction:

$$L_x = y p_z - z p_y \longleftrightarrow \hat{L}_x = -i \hbar \left\{ y \frac{\partial}{\partial z} - z \frac{\partial}{\partial y} \right\}, \quad (61)$$

energy:

$$E = \frac{p^2}{2m} + V(x) \longleftrightarrow \hat{H} = -\frac{\hbar^2}{2m} \frac{d^2}{dx^2} + V(x). \quad (62)$$

## 3. Postulate 3

When an observable, corresponding to  $\hat{A}$ , is measured, the only values observed are given by:

$$\hat{A} \Psi_n = a_n \Psi_n, \quad (63)$$

where  $a_n$  is a set of eigenvalues called the spectrum of  $\hat{A}$ . What if the system is in some arbitrary state,  $\Psi$ , which is not the eigenfunction of  $\hat{A}$ ?

## 4. Postulate 4

The expected value of  $\hat{A}$  when  $\Psi$  is not an eigenfunction of  $\hat{A}$  is given by:

$$\langle \hat{A} \rangle \equiv \int_{Space} \Psi^* \hat{A} \Psi dV. \quad (64)$$

## 5. Postulate 5

The time dependence of  $\Psi(\vec{r}, t)$  is given by the time-dependent Schrödinger equation,

$$\hat{H} \Psi(\vec{r}, t) = i \hbar \frac{\partial}{\partial t} \Psi(\vec{r}, t). \quad (65)$$

If the the hamiltonian,  $\hat{H}$ , does not include time explicitly, the wave function can be written as a product of two functions,

$$\Psi(\vec{r}, t) = \psi(\vec{r}) f(t). \quad (66)$$

As we have mention earlier this separation of variables leads to the time independent Schrödinger equation

$$\hat{H} \psi(\vec{r}) = E \psi(\vec{r}) . \quad (67)$$

The solution of Eq. 67 implies a set of energies  $\{E_n\}$  i.e.,

$$\hat{H} \psi_n(\vec{r}) = E_n \psi_n(\vec{r}) , \quad (68)$$

where  $\psi'_n$ s are called the stationary states, and each state is characterized by an energy  $E_n$ . In this sense we say that the energy is quantized.

Also we can solve the time dependent differential equation and find

$$f(t) = \exp \left\{ - i \frac{E_n t}{\hbar} \right\} , \quad (69)$$

which means that the time dependent wave function is given by the following expression:

$$\Psi(\vec{r}, t) = \psi(\vec{r}, t) \exp \left\{ - i \frac{E_n t}{\hbar} \right\} . \quad (70)$$

Since the energy is quantized, we represent an atom or molecule by a set of stationary energy states. The spectroscopic properties of the system will be understood in terms of transitions from one stationary state to another. The energy associated with the transition is equal to:

$$\Delta E_{n \rightarrow m} = E_m - E_n = h\nu , \quad (71)$$

where  $\nu$  is the frequency of the photon either emitted or absorbed.

In general the system is not going to be in a stationary state  $\psi_n$ . In this case we can ask How many atoms are in each stationary state  $\psi_n$ ? Since the system is not in a stationary state we can construct a wave function for the system as a linear combination of the stationary states  $\psi_n$ . In other words the system's wave function is given by:

$$\Phi(\vec{r}, t) = \sum_{n=1}^{\infty} C_n \psi_n(\vec{r}) \exp \left\{ - i \frac{E_n t}{\hbar} \right\} . \quad (72)$$

Therefore the probability of measuring a particular  $E_n$  value in a series of observations is proportional to the square of its coefficient  $C_n$ , i.e.,  $C^*C = |C|^2$ .

## Lecturel

### I. INTRODUCTION

For the last twenty-five years sustained oscillations of the concentration of a chemical substance have been the subject of intensive study. In spite of theoretical predictions of damped oscillations and sustained oscillations by Lotka and Hirniakand [7, 8] in 1910 and Lotka [9] in 1920, and the experimental observation of cyclic changes in the iodate catalyzed decomposition of hydrogen peroxide by Bray in 1921[10], both experimentalists and theorists virtually ignored the field of chemical oscillations. The First Symposium on Biological and Biochemical Oscillators was organized in 1968, forty seven years after Bray's paper appeared in the Journal of the American Chemical Society.

In the early 1950's Belusov [11] observed cyclic color changes in the bromination of citric acid catalyzed by cerium. However, the world scientific community did not gain access to the experimental details of these cyclic color changes, since Belusov's first findings were rejected for publication in 1951, and another six years of detailed experimentation were again rejected in 1957 [12]. Out of his work Belusov published an abstract in an obscure symposium in 1959 [11] and kept the original manuscript; he never tried again to publish his results. For years the Belusov protocol for chemical oscillations was known only to researchers and students at the Moscow State University, until one of those students, Zhabotinsky, initiated a careful and detailed investigation of the Belusov reaction during the first half of the 1960's. In the final analysis, Zhabotinsky substituted citric acid for malonic acid and published his findings in 1964 [13]. By 1967 the first paper written in English reached the West, causing immense interest among many researchers.

An interesting aspect of the Belusov-Zhabotinsky (B-Z) reaction centers around the original motivation that led Belusov to the celebrated reaction. Originally, his interest in biochemistry, and in particular in the Krebs cycle [14], motivated Belusov to seek a simple experimental model in which a carbohydrate was oxidized in the presence of a catalyst. In other words, the B-Z reaction was intended as a model of an enzyme catalyzed reaction. This connection between enzyme kinetics and the B-Z reaction is often forgotten and rarely

mentioned. Most likely, this omission can be traced to the differences between an enzyme and its model counterpart  $C_e$ , the complicated mechanism underlining the chemical oscillations in the B-Z reaction and the mathematical analyses needed to understand some of the reduced models of the B-Z reaction. From the biochemical point of view, these differences are difficult to reconcile with a biological model. Therefore, the search for a model of chemical oscillation in enzyme kinetics that is both biochemically relevant and mathematically simple enough to present to an undergraduate audience is worthwhile from the pedagogical point of view.

In the present discussion we consider glycolysis, centering around the allosteric properties of phosphofructokinase (PFK). For nearly thirty years oscillations in the concentration of nucleotides in the glycolytic pathway have been documented in the case of yeast cells and cell-free extract [15]. For example, reduced nicotinadenine dinucleotide (NADH) oscillations in yeast extract have been observed and determined to be flux dependent; a minimum external flux is required to sustain oscillations in the concentration of NADH. Moreover, Hess and Boiteux [16] observed that phosphofructokinase plays an essential role in these oscillations. If PFK's substrate, fructose-6-phosphate (F-6-P), is added to cell-free extracts, the nucleotide concentrations oscillate. On the other hand, after the injection of PFK's product, fructose-1,6-bisphosphate (F-1,6-bP), no oscillations are observed. Based on these observations and on the allosteric properties of PFK, two models were suggested in the late 1960's. One, by Higgins [17], is based on the activation of PFK by its product. The second model [18] is based on the activation and inhibition properties of PFK by adenosine triphosphate (ATP), adenosine diphosphate (ADP) and adenosine monophosphate (AMP). The latter links PFK with pyruvate kinase, while the former does not.

In the next section we discuss the steps along the glycolytic pathway which are relevant to the Higgins model. Next we reduce the model to two variables and discuss its similarities with Lotka's models and the origin of the autocatalytic step. Finally, we scale the model, do a linear stability analysis and discuss the bifurcation diagram of the reduced, two-variable Higgins model.

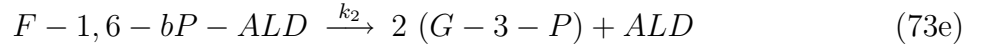
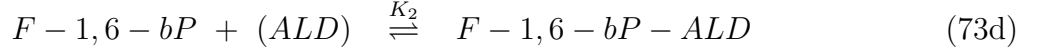
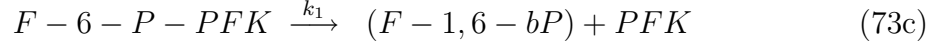
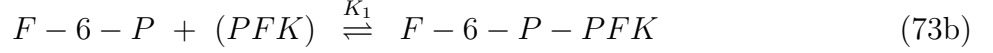
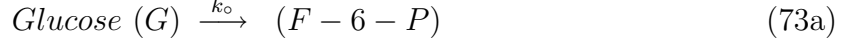
## II. HIGGINS MODEL

The interest in the origin of periodic biological processes like the circadian clock has motivated researchers to look for the chemical basis of oscillations in biochemical systems [19]-[21]. One of these systems is glycolysis, in which six-membered sugars are converted anaerobically into tricarboxylic acids. This process allows the phosphorylation of ADP. In the case of glycolysis the addition of glucose to an extract containing the main metabolites triggers cyclic, or periodic, behavior in the concentrations of metabolites. This periodic change in the concentrations of the glycolytic metabolites is termed glycolytic relaxation oscillations. In particular, relaxation oscillations in the concentration of NADH are readily observed using spectrophotometric methods on yeast extracts. For the past twenty-five years, researchers have studied mostly relaxation oscillations which are due to a single injection of glucose. In this case, the system relaxes to equilibrium. Conversely, if constant or periodic injection is applied, a system is pushed away from equilibrium and can achieve nonequilibrium steady states.

Researchers have found that phosphofructokinase (PFK), which catalyzes the conversion of F-6-P to F-1,6-bP, is the regulatory enzyme for glycolytic oscillations [22]-[23]. This regulation is the result of the activation and inhibition properties of PFK. For example, in liver, PFK is activated by F-2,6-bP [24] which is an isomer of F-1,6-bP. And in muscle, PFK is inhibited by ATP. Based on these facts, most kinetic models of glycolytic oscillations have centered around either PFK's inhibition [18] or its activation [17]. One of the models based on the activation of PFK by fructose biphosphate is the Higgins model. This model considers only two enzymatic reactions with a constant external source of glucose. Condensing two steps of the glycolytic path into one, the Higgins model assumes a first order conversion of glucose to F-6-P. Following this first step, the Higgins model considers the enzymatic conversion of F-6-P to F-1,6-bP by PFK and F-1,6-bP to glyceraldehyde-3-phosphate (G-3P) by aldolase (ALD). In this model, the regulation consists only of the activation of an inactive Phosphofructokinase ( $\overline{PFK}$ ) by F-1,6-bP. Under this assumption, the Higgins model sustains oscillations in the concentration of F-6-P, F-1,6-P and the enzymes. Using further simplifications, such as the steady-state approximation for PFK, the model reduces to three time-dependent species with autocatalytic conversion of F-6-P to F-1,6-bP. Finally, if one considers a steady-state approximation for ALD, one obtains a two-species model

which is able to sustain oscillations.

The following equations depict the steps along the glycolytic pathway that are relevant to the Higgins model:



For the sake of a simple notation, the following mechanism, which is equivalent to Eq. (73b)-(73f), will be used:



where G stands for glucose, X for F-6-P,  $E_1$  for PFK, Y for F-1,6-bP and  $E_2$  for ALD.

Using these equations, the mass action laws for the six species model are as follows:

$$\frac{d[X]}{dt} = k_o G_o - k_{E_1}^+ [E_1][X] + k_{E_1}^- [E_1 X] \quad (75a)$$

$$\frac{d[Y]}{dt} = k_1 [E_1 X] - k_{E_2}^+ [E_2][Y] + k_{E_2}^- [E_2 Y] - k_a^+ [\overline{E}_1][Y] + k_a^- [E_1] \quad (75b)$$

$$\frac{d[E_1]}{dt} = k_{E_1}^- [E_1 X] - k_{E_1}^+ [E_1][X] + k_1 [E_1 X] - k_a^- [E_1] + k_a^+ [\overline{E}_1][Y] \quad (75c)$$

$$\frac{d[E_1 X]}{dt} = -k_{E_1}^- [E_1 X] + k_{E_1}^+ [E_1][X] - k_1 [E_1 X] \quad (75d)$$

$$\frac{d[E_2]}{dt} = k_{E_2}^- [E_2 Y] - k_{E_2}^+ [E_2][Y] + k_2 [E_2 Y] = -\frac{d[E_2 Y]}{dt} . \quad (75e)$$

Using the steady-state approximation for all of the enzymes, we obtain a minimal two

variable model [25]

$$\frac{d[X]}{dt} = k_o G_o - k_{ac}[X][Y] \quad (76a)$$

$$\frac{d[Y]}{dt} = k_{ac}[X][Y] - \frac{V_{2m} \frac{[Y]}{K_{2M}}}{1 + \frac{[Y]}{K_{2M}}} \quad (76b)$$

where  $k_{ac}$  is given by the following equation:

$$k_{ac} = \frac{K_a \frac{V_{1m}}{K_{1M}}}{1 + K_a[Y] + \frac{K_a}{K_{1M}}[X][Y]} \quad (77a)$$

$$K_{iM} = \frac{k_i + k_{E_i}^-}{k_{E_i}^+} \quad (77b)$$

$$V_{im} = k_i E_i^\circ \quad (77c)$$

$$K_a = \frac{k_a^+}{k_a^-} \quad (77d)$$

$$(77e)$$

In Eq.(77d)  $E_i^\circ$  represents the stoichiometric concentration of the  $i^{th}$  enzyme. Also in the Higgins model,  $k_{ac}$  is simplified even further to

$$k_{ac} = \frac{V_{1m} K_a}{K_{1M}} = \frac{k_1 k_{E_1}^+ E_i^\circ K_a}{k_1 + k_{E_1}^-} \quad (78)$$

Equations (76b)-(78) constitute the Minimal Higgins (MH) model .

### A. Comparison with the Lotka Model

The Minimal Higgins Model as expressed by Eqs. (76b) and (76b) shows some similarities with the Lotka's models. For example, in the original Lotka model of 1910, species reproduction is proportional to the amount of food, which is kept constant; namely



This elementary step, in conjunction with the following steps:



define what is known as the Lotka Model and the differential equations describing the time behavior of the population are given in Table I.

<b>Table I</b>	
<b>Model</b>	<b>Differential equations</b>
<b>Lotka 1910</b>	$\frac{d[R]}{dt} = k_R G_o - k_W [R][W]$ $\frac{d[W]}{dt} = k_w [R][W] - k_D [W]$
<b>Lotka 1920</b>	$\frac{d[R]}{dt} = k_R G_o [R] - k_W [R][W]$ $\frac{d[W]}{dt} = k_w [R][W] - k_D [W]$
<b>Minimal Higgins</b>	$\frac{d[X]}{dt} = k_o G_o - k_{ac}[X][Y]$ $\frac{d[Y]}{dt} = k_{ac}[X][Y] - \frac{V_{2m}[Y]}{K_{2M} + [Y]}$
<b>Schankenberg</b>	$\frac{d[X]}{dt} = k_o G_o - k_S [X][Y]^2$ $\frac{d[Y]}{dt} = k_s [X][Y]^2 - k_D [Y]$

Notice that the first differential equations in the MH model and the Lotka's 10 model are the same. In the 1920 paper, Lotka introduced a species dependent external flux, namely



which is a autocatalytic step and substitutes Eq.(79). In this case, the differential equations describing the time behavior of the populations are given in Table I. In both Lotka's models cases, the concentration of grass,  $G_o$ , is kept constant. Notice that the 1920 model is a variation of the 1910 model which yields oscillation in the population. Consequently, we

can think of the MH model as a variation of the 1910 model where we have included an enzymatic step instead of a first order step.

These two Lotka models are the simplest schemata in which oscillations in the populations can be observed. A meaningful interpretation of this model is in population dynamics. For example if we define G as grass, R as rabbit and W as wolf, the explanation of the oscillatory behavior seems quite logical. As the rabbits consume the grass and reproduce, their numbers grow, while the amount of grass decreases. As the rabbit population grows, the wolves have plenty of rabbits available for consumption, and they, too, reproduce. However, as the wolf population increases, the rabbit population decreases. As the rabbit population decreases, the wolves start to die, since there are not enough rabbits. As a consequence, grass becomes more plentiful, and the rabbits start the cycle again. Unfortunately, the first Lotka model yields only damped oscillation and the second model gives sustained oscillations for any initial condition, which is a severe restriction if we want to model realistic chemical and biochemical system. In contrast, the Minimal Higgins model shows stable steady states, damped and sustained oscillations. The richness of this model stems from the second differential equation which includes an enzymatic Michaelis-Menten step. Moreover, the autocatalytic step in the MH model can be traced to the activation of PFK by its product. The fourth model in Table I is due to Schnakemberg [28]. In this model, the bimolecular autocatalytic step in the Lotka 1910 model is replaced by a trimolecular step. This change appears as a cubic term in the differential equations. With this change, the model shows sustained oscillations. But the connection between the cubic autocatalytic term and a biochemical justification has not been achieved.

### III. STABILITY ANALYSIS

In this section we present a linear stability analysis [26] of the Minimal Higgins model. For this purpose, we scale the differential equation such that the dimensionless differential equations depend only on two parameters rather than on five. Namely, we get from Eqs. (76b)-(76b)

$$\frac{dX}{d\tau} = A - XY \tag{82a}$$

$$\frac{dY}{d\tau} = XY - \frac{qY}{1+Y} \ , \tag{82b}$$

where we have defined the following dimensionless quantities:

$$\tau = k_{ac}K_{2M}t \quad (83a)$$

$$X = \frac{[X]}{K_{2M}} \quad (83b)$$

$$Y = \frac{[Y]}{K_{2M}} \quad (83c)$$

$$A = \frac{k_o G_o}{K_{2M}^2 k_{ac}} \quad (83d)$$

$$q = \frac{V_{2m}}{K_{2M}^2 k_{ac}} \quad (83e)$$

The first step in the stability analysis is to find the steady state solution. In general this is done by setting the left hand side of the differential equations equal to zero and solving for the concentrations. From Eqs.(82b)-(82b), we obtain for the scaled MH model the following steady state solutions:

$$x^{ss} = q - A \quad (84a)$$

$$y^{ss} = \frac{A}{q - A} \quad (84b)$$

Clearly from Eqs.(84b)-(84b), we can see that the physically meaningful solutions have to satisfy the following condition:  $q > A$ . Only values of A less than q give meaningful physical results, i.e.,  $x^{ss}$  and  $y^{ss}$  have to be positive.

Once these stationary states are obtained, stability analysis studies what happens to all components of the system when the system is perturbed slightly from its steady state. For this purpose we first calculate the relaxation matrix, R, which is the Jacobian associated to a set of ordinary differential equations (ODEs) [26]. For the scaled MH model, we obtained the following matrix:

$$R = \begin{pmatrix} -y^{ss} & -x^{ss} \\ y^{ss} & x^{ss} - \frac{q}{(1+y^{ss})^2} \end{pmatrix} \quad (85)$$

Next, we have to find the eigenvalues,  $\lambda_{\pm}$  of R, which are the solutions of the following characteristic polynomial:

$$\lambda^2 + \left[ \frac{(1+y^{ss})(y^{ss}-x^{ss})+x^{ss}}{1+y^{ss}} \right] \lambda + \left[ \frac{x^{ss}y^{ss}}{1+y^{ss}} \right] = 0 \quad (86)$$

In this case the solutions of the quadratic Eq.( 86) are

$$\lambda_{\pm} = -\frac{1}{2} \left[ \frac{(1+y^{ss})(y^{ss}-x^{ss})+x^{ss}}{1+y^{ss}} \right] \pm \frac{1}{2} \sqrt{\left[ \frac{(1+y^{ss})(y^{ss}-x^{ss})+x^{ss}}{1+y^{ss}} \right]^2 - 4 \left[ \frac{x^{ss}y^{ss}}{1+y^{ss}} \right]} \quad (87)$$

Equation (87) can be reduced to the following expression:

$$\lambda_{\pm} = \frac{P_R(A, q) \pm \sqrt{P_I(A, q)}}{2q(q - A)}, \quad (88)$$

where we have defined the following functions:

$$P_R(A, q) = A [A^2 - 2Aq + q^2] \quad (89)$$

$$P_I(A, q) = A [A^5 - 4qA^4 + 2q(3q + 1)A^3 - 4q^2(q + 2)A^2 + q^2(q^2 + 10q + 1)A - 4q^2] \quad (90)$$

Equations (89,90) have been obtained both by analytical methods and with the help of the software package MATHEMATICA [27].

From Eqs.(87)-(90) , we can analyze four possible eigenvalues: a)  $P_R < 0$  and  $P_I > 0$ . In this case, the eigenvalue is pure real and negative. Thus the steady state solution is a stable fixed point [26]. b)  $P_R < 0$  and  $P_I < 0$ . In this case, the eigenvalue has a negative real part and a nonzero imaginary part. For this eigenvalue, we find damped oscillations. c)  $P_R > 0$  and  $P_I > 0$ . In this case, the eigenvalue is pure real and positive. The steady state is unstable. d)  $P_R > 0$  and  $P_I < 0$ . In this case, the eigenvalue has a positive real part and a nonzero imaginary part. The steady state is unstable and moves away to unstable oscillations.

Also, we can construct a plot of A vs. q. Figure 1, depicts such a diagram, and the different lines represent curves where A - q,  $P_R$  and  $P_I$  are equal to zero. These curves delimit different regions in parameter space. In region A, we observe stable fixed points, in region B, we observe damped oscillations, and region C, we observe sustained oscillations.

For a fixed value of q, the value of A at which  $P_R(A, q)$  is equal to zero,  $A_c$ , defines the bifurcation point. Values of A greater than  $A_c$  are in regions A or B, and for values less than  $A_c$  are in region C. Thus for  $A_c < A < q$  the system reaches a fixed point e.g. Figure 2 and 3. For  $A < A_c$ , the systems reaches a limit cycle e. g. Figure 4. The diagram of A versus oscillation amplitude is called a bifurcation diagram [26] depicted by Figure 5.

The only problem with the Minimal Higgins model is a fixed point at  $y = 0$  and an infinite large value of  $x$ . For a fixed q this case occurs for small values of A, where also numerical integration becomes problematic. For this reason the bifurcation diagram only considers values of A greater than 2. This particular problem is also present in the Lotka's models as well as in the Schnakenberg model [28].

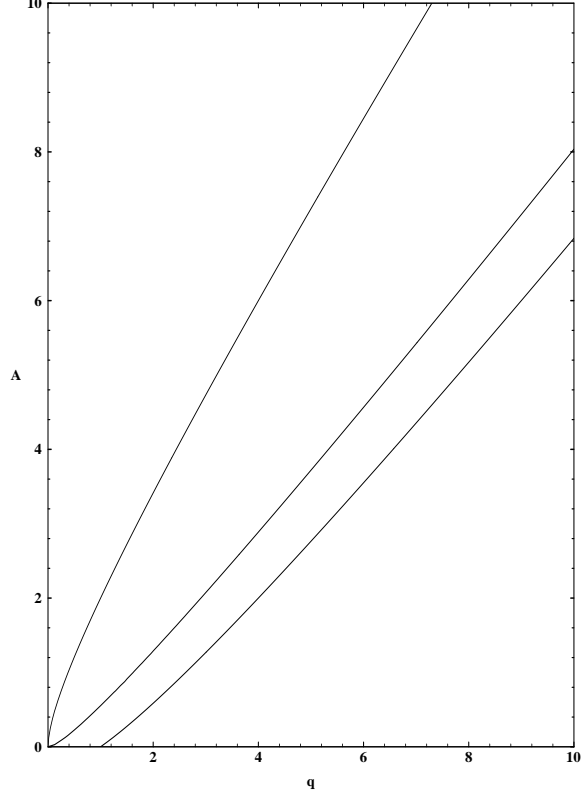


FIG. 2: Parameter space diagram for the Minimal Higgins model. Region A is limited by the line  $q = A$  and  $P_R(A, q) = 0$ ; Region B is limited by  $P_R(A, q) = 0$  and  $P_I(A, q) = 0$ ; Region C is defined by  $P_I(A, q) > 0$ .

#### IV. SUMMARY

The minimal Higgins model is a simple two species model that shows sustained oscillations in enzyme kinetics. The steps in the mechanism have a biochemical justification and the step responsible for the oscillation is a Michaelis-Menten step. Also, the stability analysis is simple and accessible both analytically or with the help of MATHEMATICA. For example the bifurcation points are obtained by fixing either A or q and solving a simple quadratic equation, e.g. Equation(89).

The only problem associated with the MH model and inherent to all of the models in Table I is a fixed point at  $y = 0$  and an infinite large value of  $x$ . Numerically and for fixed q, the problem appears for small values of A. In some cases, MATHEMATICA is not able to handle the numerical integrations and other algorithms are required to study the differential

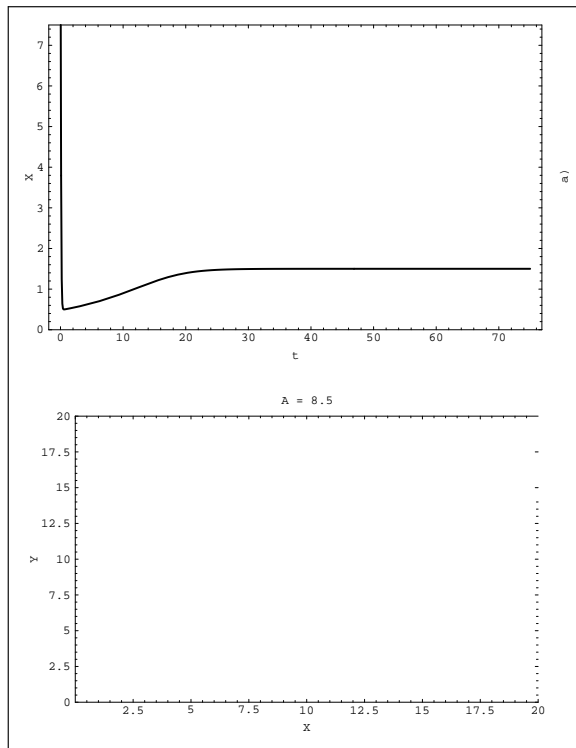


FIG. 3: Example from region A. In this case  $q = 10$  and  $A = 8.50$ . a)  $x$  vs  $t$ ; b)  $x$  vs.  $y$ .

equations for small values of  $A$  [? ?]. Modification intended to remove this kind of fixed points have been done for the Schnakenberg model. For example, the addition of a first order conversion of  $x$  into  $y$  i.e.



yield the two-variable autocatalator model. Also, the well known Brusselator can be obtained from the Schnakenberg model by replacing the first order formation of  $X$  by



Although these models do not have fixed points at infinity, a biochemical justification for those steps does not exist. In the case of the MH model similar modifications can be done to remove the fixed point at infinity. In these case, the modification have a plausible

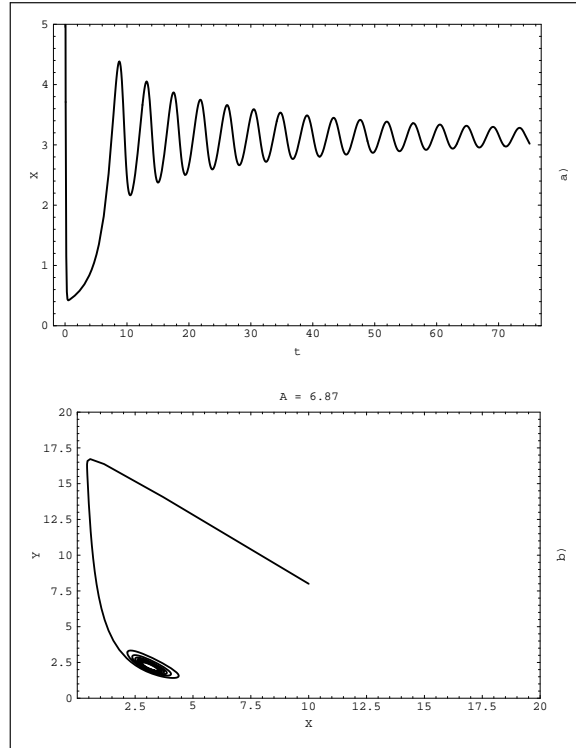


FIG. 4: Example from region B. In this case  $q = 10$  and  $A = 6.87$  a)  $x$  vs  $t$ ; b)  $x$  vs.  $y$ .

explanation. For example, synthesis of glycogen could prevent infinitely large values of  $X$ . And from high levels of glycogen, an eventual formation of F-1,2-bP can be assume. These two steps have the equivalent effect as Eq. (91).

In summary, the Minimal Higgins model provides us with a simple system of non-linear differential equations that can be biochemical justified. Also, the model's stability analysis is easy to handle both analitically or with the help of MATHEMATICA. This yields simple study of the bifurcation diagrams.

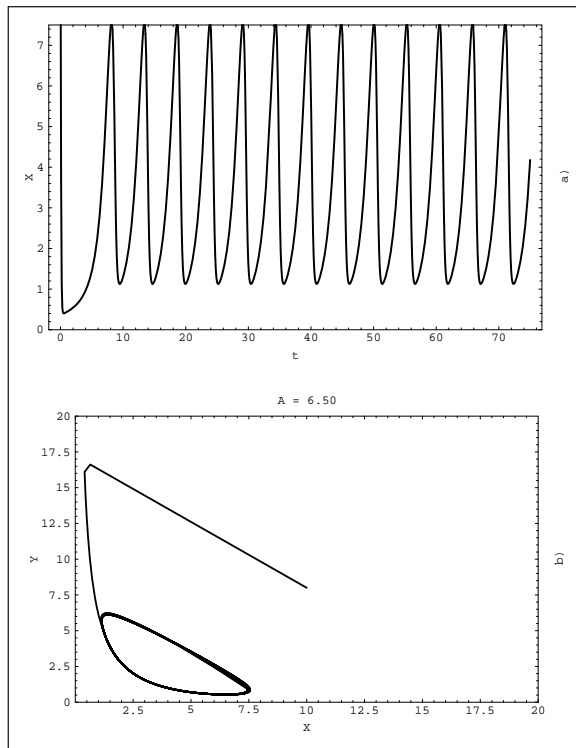


FIG. 5: Example from region C. In this case  $q = 10$  and  $A = 6.50$ . a)  $x$  vs  $t$ ; b)  $x$  vs.  $y$ .

## V. GENERAL MODEL

In previous work [?]–[?] we have considered Rebek’s self-replicating system and modeled ideal self-replication using a self-complementary template mechanism. For this mechanism we used a reasonable chemical model that is consistent with the laboratory work on self-replication. In particular, we have focused on a simple self-replicating mechanism; however, in general, chemical self-replication can be represented schematically by the following mechanistic steps:

where  $T$  represents the self-replicating molecule and  $A$  and  $B$  are the component fragments. In the uncatalyzed step, components  $A$  and  $B$  “collide” with a relative low probability to form the template,  $T$ . The structure of the product  $T$  is such that once it is formed, it preferentially binds  $A$  and  $B$  in a conformation that facilitates covalent bonding between the  $A$  and  $B$  molecules to form another  $T$  molecule. The newly created template and the original template molecules then split apart and independently catalyze further reactions.

While considering ideal self-replication, we have coupled the autocatalytic process with an enzymatic removal sink of the template



where the rate shows saturation at high concentrations of  $T$ .

Elsewhere [?]–[?] we have shown that the mechanism illustrated by Eqs. (??) can be reduced to a two-variable system. Here we extend the case of the ideal self-replicator to include the square root rate law as well as other orders. The dynamics of this extended model in time and space are defined by the following pair of dimensionless partial differential equations:

$$\frac{d u}{d t} = k_o u_o - k_u u^2 - k_t u^2 v, \quad (95a)$$

$$\frac{d v}{d t} = k_u u^2 + k_t u^2 v - \frac{q(T) v}{K_M + v}, \quad (95b)$$

$$C_P V \frac{d T}{d t} = \Delta H V \frac{q(T) v}{K_M + v} - S A (T - T_o). \quad (95c)$$

where

$$q(T) = q(T_o) \exp\left(-\lambda \left(\frac{1}{T} - \frac{1}{T_o}\right)\right) \quad (96)$$

in which  $d = D_2/D_1$  is the ratio of the diffusion coefficients. The parameters  $r$ , which characterizes the external input in the chemical pool approximation, and  $K$ , which characterizes the enzymatic sink, are the relevant parameters in our analysis. The other parameter,  $\beta$ , is either unity or zero. In the former case the system has an enzymatic removal and in the latter case the system has a linear removal. Also, in self-replicating chemical systems the uncatalyzed process occurs with a very low probability, so  $k_u \ll 1$ . For details see references [? ?]. Finally, notice that for  $k_u = 0$  and  $\beta = 0$  we recover Lotka’s 1910 model [7] if we select  $m = 1$  and  $n = 1$  and the Autocatalator [18]–[?] if  $m = 1$  and  $n = 2$ . In contrast, if  $\beta = 1$  we recover the Higgins model [15]–[?] for  $k_u = 0$ ,  $m = 1$  and  $n = 1$  and the Templator [?]–[?] for  $m = 2$  and  $n = 1$ .

## A. Temporal Patterns

To study temporal patterns of the self-replicating system given by Eqs. (95) we must consider a spatially homogeneous system, so we eliminate the Laplacian from Eq. (95). To

find the conditions for chemical oscillations, we first find the steady state  $(\bar{u}, \bar{v})$  of Eq. (95),

$$\bar{v} = \frac{r K}{1 - \beta r} , \quad (97a)$$

$$\bar{u} = \left( \frac{r}{k_u + \bar{v}^n} \right)^{\frac{1}{m}} , \quad (97b)$$

where we notice that, since  $\bar{v} > 0$ ,  $\beta r < 1$ . This condition reduces the size of the parameter space considerably.

Next we reduce the Jacobian to the following form:

$$J = \begin{pmatrix} -\frac{m r}{\bar{u}} & -\frac{n r}{\bar{v}} + k_u \frac{n \bar{u}^n}{\bar{v}} \\ \frac{m r}{\bar{u}} & \frac{(n-1)r + \beta r^2}{\bar{v}} - k_u \frac{n \bar{u}^n}{\bar{v}} \end{pmatrix} , \quad (98)$$

and calculate the determinant of the Jacobian at the steady state.

$$\begin{aligned} \det J_{\bar{u}, \bar{v}} &= m \frac{r^2}{\bar{u} \bar{v}} (1 - \beta r) = \\ &= \frac{m r^2 (1 - \beta r)^2 [K^n r^n + k_u (1 - \beta r)^n]^{1/m}}{K r^{\frac{1+m}{m}} (1 - \beta r)^{\frac{n}{m}}} \geq 0 . \end{aligned} \quad (99a)$$

Since  $\beta r < 1$ , the determinant of the Jacobian at the steady state is always positive for all non-zero  $m$  and all  $n$ , and thus the stability of the steady states is determined by the sign of the trace of the Jacobian.

The trace of the Jacobian evaluated at the steady state is given by a somewhat more complicated expression,

$$\text{tr} dJ_{\bar{u}, \bar{v}} = \frac{F}{K [K^n r^n + k_u (1 - \beta r)^n] (1 - \beta r)^{\frac{n}{m}}} , \quad (100a)$$

where we have defined

$$\text{tr} dJ_{\bar{u}, \bar{v}} \equiv d J_{11} + J_{22} \quad (100b)$$

and

$$\begin{aligned} F &\equiv [(n - 1 - \beta r) K^n r^n - k_u (1 - \beta r)^{n+1}] (1 - \beta r)^{\frac{m+n}{m}} \\ &- (m d) K r^{\frac{m-1}{m}} [K^n r^n + k_u (1 - \beta r)^n]^{\frac{m+1}{m}} . \end{aligned} \quad (100c)$$

Notice that in Eq. (100b) we have included the dimensionless diffusion coefficient  $d$ . In this section we will consider the case  $d = 1$ , but for spatial patterns we must analyze Eq. (100b) with  $d < 1$ .

Depending on the relative sizes the terms in Eq. (100c), the trace may be positive or negative. In particular we are interested in finding when, for  $d = 1$ , the trace greater or equal to zero, so we consider the following equation:

$$\begin{aligned} & [(n-1 + \beta r)K^n r^n - k_u(1 - \beta r)^{n+1}] (1 - \beta r)^{\frac{m+n}{m}} - \\ & (m)K r^{\frac{m-1}{m}} [K^n r^n + k_u(1 - \beta r)^n]^{\frac{m+1}{m}} \geq 0 . \end{aligned} \quad (101)$$

The inequality in Eq. (101) implies that the steady state is unstable and therefore small homogeneous perturbations grow over time. The equality, which we can rewrite as

$$K = \frac{(1 - \beta r) \left[ (n-1 + \beta r) - k_u \frac{(1-\beta r)^{n+1}}{K^n r^n} \right]^{\frac{m}{m+n}}}{m^{\frac{m}{m+n}} r^{\frac{m+n-1}{m+n}} \left[ 1 + k_u \frac{(1-\beta r)^n}{K^n r^n} \right]^{\frac{m+1}{m+n}}} , \quad (102)$$

defines an exact transcendental equation that, when solved for  $K$ , yields a Poicare-Adronov-Hopf (PAH) bifurcation.

Notice that for  $k_u = 0$  we obtain an exact analytical solution for the PAH bifurcation for any values of  $m$  and  $n$  provided  $(n-1 + \beta r) \geq 0$ . Another relevant limiting case is the linear removal in Eqs. (95) that we recover when  $\beta = 0$  and  $K = 1$ , which yields the following bifurcation relation:

$$K_{bif} = \frac{[n-1]^{\frac{m}{m+n}}}{m^{\frac{m}{m+n}} r^{\frac{m+n-1}{m+n}}} . \quad (103)$$

From Eq. (101) we need that  $(n-1) \geq 0$ . This last constraint requires a value of  $n$  greater than unity. Therefore the smallest nonlinearity coupled with a linear sink that is able to sustain oscillations is the so-called Autocatalator, in which  $m = 1$  and  $n = 2$ .

In contrast, when  $\beta = 1$  we get an enzymatic sink in Eq. (95), and for  $k_u = 0$  we get the following analytical bifurcation relation:

$$K_{bif} = \frac{(1-r) [(n-1+r)]^{\frac{m}{m+n}}}{m^{\frac{m}{m+n}} r^{\frac{m+n-1}{m+n}}} , \quad (104)$$

in which  $(n-1+r) \geq 0$ . Notice that  $n$  no longer has to be greater than unity in a system with  $m$  and  $n$  greater than zero. As long as  $(n-1+r) \geq 0$ , the system shows a PAH bifurcation. For example, for  $\beta = 1$ ,  $m = 2$  and  $n = 1$  we recover the Templator model with a cubic nonlinearity and for  $\beta = 1$ ,  $m = 1$ , and  $n = 1$  we recover the Higgins model which contains a quadratic nonlinearity.

Moreover, for  $\beta = 1$ ,  $m = 1/2$  and  $n = 1/2$ , the system with nonlinearity  $m+n = 1$  shows oscillations if

$$K \leq (1-r) \sqrt{2r-1} , \quad (105)$$

where  $1/2 \leq r \leq 1$ . In summary, the inclusion of an enzymatic sink instead of a linear sink in Eq. (95) allows the systems with nonlinearities less than cubic to sustain oscillations.

Since we already derived a general bifurcation condition for this system in terms of the parameters and  $m$  and  $n$ , to obtain a bifurcation diagram for the generalized model, we simply set  $m = 1$ ,  $n = 1/2$ ,  $k_u = 0.01$  and  $\beta = 1$  and then plot the bifurcation condition given by Eq. 102 to visualize the relationship between  $K$  and  $r$ . In Figure (??A) we depict the curve  $\text{tr } J = 0$ , in which, for a given value of  $K$ , we can find two PAH bifurcation points as we vary  $r$ . In addition, if the parameter values fall within the loop, the trace of the Jacobian at the steady state is positive and thus the system is capable of stable oscillatory solutions.

We repeat our analysis for  $m = 2$  and in Figure (??B) we plot the PAH bifurcation curve. Notice that here the area of the region in which  $\text{tr } J > 0$  is smaller than when  $m = 1$ . Thus when  $m = 2$  oscillations are restricted to a smaller set of parameter values

## B. Spatial Patterns

Next we consider heterogeneous perturbations which result when  $d < 1$  and find the conditions for Turing patterns, which are a kind of spatial pattern. [?]–[?] In general, for a system to sustain Turing patterns the following four conditions must be satisfied:

$$\det J > 0 , \tag{106a}$$

$$J_{11} + J_{22} < 0 , \tag{106b}$$

$$d J_{11} + J_{22} > 0 , \tag{106c}$$

$$(d J_{11} + J_{22})^2 > 4 d \det J , \tag{106d}$$

where  $J$  is the Jacobian and  $J_{11}$  and  $J_{22}$  are the diagonal elements of the Jacobian.

As discussed earlier, the determinant is always positive for physical parameter values, so we only need to consider the final three conditions. We have already calculated expressions for second and third inequalities in the previous section. The fourth relation yields the

following equation:

$$\begin{aligned}
& (md)Kr^{\frac{m-1}{m}} [K^n r^n + ku(1-\beta r)^n]^{\frac{m+1}{m}} + \\
& 2\sqrt{Kmd} r^{\frac{m-1}{2m}} [K^n r^n + ku(1-\beta r)^n]^{\frac{2m+1}{2m}} (1-\beta r)^{\frac{2m+n}{2m}} \\
& - (n-1+\beta r)K^n r^n (1-\beta r)^{\frac{m+n}{m}} + \\
& ku(1-\beta r)^{2+n+n/m} < 0.
\end{aligned} \tag{107}$$

For the minimal case  $k_u = 0$  the last three Turing conditions reduce to the following analytical expressions, respectively:

$$K > \frac{(1-\beta r)(n-1+\beta r)^{\frac{m}{m+n}}}{(m)^{\frac{m}{m+n}} r^{\frac{m+n-1}{m+n}}} \tag{108a}$$

$$K < \frac{(1-\beta r)(n-1+\beta r)^{\frac{m}{m+n}}}{(m d)^{\frac{m}{m+n}} r^{\frac{m+n-1}{m+n}}} \tag{108b}$$

$$K < \frac{(1-\beta r)(\sqrt{n}-\sqrt{1-\beta r})^{\frac{2m}{m+n}}}{(m d)^{\frac{m}{m+n}} r^{\frac{m+n-1}{m+n}}} \tag{108c}$$

Moreover, the intersection of the PAH bifurcation and the Turing conditions defines a codimension-two point where both the PAH and the Turing conditions are satisfied. This point is easily calculated from Eqs. (108).

$$r_c = \frac{1}{\beta} \left[ 1 - \left( \frac{1-d}{1+d} \right)^2 n \right], \tag{109}$$

where the critical value of  $r$  depends only on  $d$  and  $n$  and is independent of  $m$ .

To find the bifurcation diagrams that illustrate the parameter values required for Turing patterns, we first numerically solve Eqs. (106) and (107) for  $k_u \neq 0$ ,  $n = 1/2$  and either  $m = 1$  or  $m = 2$ .

In Figure (??) we depict Eqs. (106) with curves  $C_1$  and  $C_2$ . Curve  $C_1$ , as in the previous section, determines the PAH bifurcation. Curve  $C_2$  is similar to  $C_1$  but was calculated with  $d = 0.20$  instead of  $d = 1$ . The region between these curves is stable to homogeneous perturbations. The fourth condition, Eq. (107), which is depicted by curve  $C_3$ , delimits the region that is unstable to inhomogeneous perturbations; therefore, points in parameter space between curves  $C_3$  and  $C_1$  satisfy necessary conditions for Turing patterns.

## Acknowledgments

The authors would like to thank the National Science Foundation for their financial support through grant CHE-0136142 and CHE-0548622.

---

- [1] L. E. Orgel, *Nature* **358**, 203 (1992).
- [2] L. E. Orgel, *Acc. Chem. Res.* **28**, 109 (1995).
- [3] T. R. Cech, *PNAS* **83**, 4360 (1986).
- [4] T. R. Cech, *Nature* **339**, 507 (1989).
- [5] G. von Kiedrowski, *Angew Chem.* **25**, 932 (1986),
- [6] B. Bag and G. von Kiedrowski, *Pure Appl. Chem.* **68**, 2145 (1996).
- [7] Lotka, A. J. *J. Am. Chem. Soc.* **1910**, 42, 1595-99.
- [8] Hirniak, Z. *Z. Physik. Chem.* **1910**, 675-680.
- [9] Lotka, A. J. *J. Phys. Chem.* **1920**, 14, 271-74.
- [10] Bray, W. C. *J. Amer. Chem. Soc.* **1921**, 43, 1262-1267.
- [11] Belusov, B. P., *Sb. Ref. Radiats. Med. za 1958.*; Medgiz: Moscow **1959**, 1, 145.
- [12] Winfree, A. T. *J. Chem Edu.* **1984** , 61, 661-663 (1984)
- [13] Zhabotinsky, A. M. *Biofizika* **1964**,9 , 306. (in Russian).
- [14] van Holde, M. *Biochemistry*; Benjamin: Redwood,1990.
- [15] Gosh, A.; Chance, B. *Biochem. Biophys. Res. Commun.* **1964**, 16, 174-81.
- [16] Boiteux, A.; Hess, B.; Sel'kov E. E. *Current Topics in Cellular Regulation* **19xx**, 17, 171-203.
- [17] Higgins, J. *Proc. Nat. Acad. Sci. U.S.* **1964**, 52, 989.
- [18] Sel'kov, E. E., *Europ.J. Biochem.* **1968**, 4, 79.
- [19] Banks, H. T. *Modeling and Control in the Biomedical Sciences*; Springer: Berlin, 1975.
- [20] Palmer, J. D., *An Introduction to Biological Rhythms*; Academic: New York, 1976.
- [21] Berridge, M. J.; Rapp, P. E.; and Treherne, J. E., Eds. *Cellular Oscillators*; Cambridge: Cambridge, 1979.
- [22] Tornhein, K. *J. Theo. Biol.* **1979**, 79, 491-541 (1979).
- [23] Tornhein, K. *J. Biol. Chem.* **1988**, 263, 2619-2624.
- [24] Pilkins, S. J.; GranmerD. K. *Annu. Rev. Physiol.* **1992**, 54, 885-909.

- [25] Ibañez, J.L.; Fairém and Velarde, M. G. *Phys. Lett.* **1976**, 58A, 364.
- [26] Edelstein-Keshet, L. *Mathematical Models in Biology*; Random: New York, 1988.
- [27] Wolfram, S., *MATHEMATICA Ver. 2.1*, Wolfram Research (1991).
- [28] Schnakenberg, J. *J. Theo. Biol.* **1979**, 81, 389-400.